Characterization of Shielded Coplanar Type Transmission Line Junction Discontinuities Incorporating the Finite Metallization Thickness Effect

Chih-Wen Kuo and Tatsuo Itoh, *Fellow, IEEE*

***Abstract*—Frequency-dependent characteristics of shielded junction discontinuities between coplanar type transmission lines, coplanar waveguide (CPW) and finline, are analyzed by the mode-matching technique. Effect of finite metallization thickness is also incorporated in the analysis for the first time. Scattering parameters of finline step discontinuity are compared with existing data to confirm the accuracy of the approach. Numerical results for finline step discontinuity, shielded CPW step discontinuity and CPW-finline transition are presented.**

I. Introduction

JUNCTION discontinuities between enclosed planar transmission lines have been analyzed by many researchers with different full-wave analysis approaches in the past. Jansen used a generalized algorithm based on the spectral-domain method [1] for the analysis of planar microwave and millimeter wave transmission line end effects [2]. Several papers based on this approach were published on the characterization of different finline discontinuities [3]–[5] and enclosed microstrip line discontinuities [6]–[8]. Another rigorous full-wave analysis approach based on the transverse resonance method [9] has also been applied to analyze the finline discontinuities [10]–[12]. The boundary value problem is formulated in terms of rectangular waveguide modes along with a proper modelling of the electromagnetic fields on the metallization plane. Computation of the higher-order finline modes is not necessary in this approach. It is worth mentioning that the formulations of the field analysis in Jansen's generalized spectral-domain approach [2] and those in [10]–[12] which use the transverse resonance method are essentially the same. The mode-matching technique [13] is an application of the moment method in which the eigenmodes of the transmission lines on both sides of the junction discontinuity are used for the basis and testing functions. This approach has also been widely used to characterize the step discontinuities of enclosed microstrip lines [14]–[17] and finlines [18]–[21].

Despite the large number of publications about the enclosed microstrip line and finline junction discontinuities, only very limited amount of data concerning shielded coplanar waveguide (CPW) discontinuities were available [22], [23]. Coplanar waveguide was suggested as an alternative to microstrip line for microwave circuits [24] because of its low frequency dispersion and easy adaptation to shunt elements. The uniplanar circuit configurations based on CPW as a circuit structure for monolithic microwave integrated circuits (MMIC) have been developed [25]. Accurate characterization of CPW junction discontinuities is hence important in MMIC design. Another effect which has been missing in previous numerical results for discontinuities obtained from full-wave analysis is the consideration of the finite metallization thickness. It is evident that the effect of metallization thickness becomes more important in the higher frequency range when the wavelength is smaller. Neglecting the effect of finite metallization thickness in MMIC design may result in substantial inaccuracy because the dimensions of the circuit are so comparable to the wavelength and the thickness of the metallization becomes significant.

This paper presents a method for characterizing the junction discontinuities between coplanar type transmission lines, specifically, shielded CPW and finline, by also considering the effect of finite metallization thickness of each individual line. The discontinuity structures which will be analyzed are the shielded CPW step discontinuity (Fig. 1(a)), finline step discontinuity (Fig. 1(b)) and the CPW-finline transition (Fig. 1(c)). The CPW step discontinuity can be used as an impedance transformation and the CPW-finline transition is the building block of microwave balanced-unbalanced mixer circuit [26], [27]. With the success of the mode-matching technique for the analysis of discontinuous structures without metallization thickness in the past, this approach is employed in this paper to formulate the boundary value problem of junc-

Manuscript received May 3, 1991; revised July 9, 1991. This work was supported by the Army Research Office under contract DAAAL03-88-K-005.

C.-Wen Kuo is with the Department of Electrical and Computer Engineering, University of Texas at Austin, Austin, TX 78712.

T. Itoh is with the Department of Electrical Engineering, University of California, Los Angeles, 405 Hilgard Avenue, Los Angeles, CA 90024-1594.

IEEE Log Number 9103897.

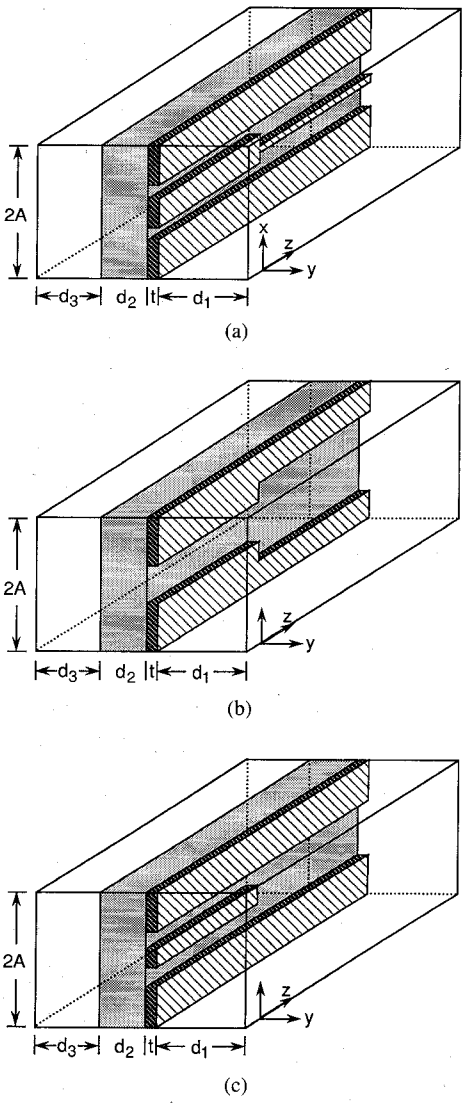

Fig. 1. Coplanar type transmission line junction discontinuities with finite metallization thickness. (a) CPW step discontinuity. (b) Finline step discontinuity. (c) CPW-finline transition. The dielectric substrate is placed symmetrically inside the rectangular waveguide.

tion discontinuities between coplanar type transmission lines. Electromagnetic fields on both sides of the discontinuity are expanded by the eigenmodes of each transmission line. The accuracy of the mode-matching technique depends primarily on the accuracy of the eigenmodes. These eigenmodes (propagating and evanescent) are calculated by using an extension of the spectral domain approach which takes into account the finite thickness of the metallization and the edge condition [28], [29].

Numerical results for finline step discontinuity without metallization thickness are first compared with existing data to confirm the accuracy of the proposed approach. Frequency-dependent scattering parameters of shielded CPW step discontinuity, finline step discontinuity and CPW-finline transition are presented for the first time, with the finite metallization thickness being considered. Effect of the metallization thickness on the scattering parameters is also studied.

II. Formulations of Eigenmodes with Finite Metallization Thickness

The formulation procedure for eigenmodes with finite metallization thickness is described for the CPW, but the approach itself is very general and can also be applied to finline. Fig. 2 shows a CPW with finite metallization thickness inside a rectangular waveguide shielding with perfect electric conducting walls. Due to the symmetry at the plane $x = 0$, only one half of the structure is considered. Electromagnetic fields in each region i, ($i = 1, 2, 3, 4$) can be written as

$$E_{yi}(x, y, z) = \frac{1}{j\omega\epsilon_i} \sum_{n=1}^{\infty} K_n^A I_{ni}^e(y) \sin \alpha_n^A(x + A) e^{-j\beta z} \tag{1a}$$

$$H_{yi}(x, y, z) = \frac{-1}{j\omega\mu_0} \sum_{n=1}^{\infty} K_n^A V_{ni}^h(y) \cos \alpha_n^A(x + A) e^{-j\beta z} \tag{1b}$$

$$E_{xi}(x, y, z) = \sum_{n=1}^{\infty} \frac{1}{K_n^A} [\alpha_n^A V_{ni}^e(y) + j\beta V_{ni}^h(y)] \cdot \cos \alpha_n^A(x + A) e^{-j\beta z} \tag{1c}$$

$$H_{xi}(x, y, z) = \sum_{n=1}^{\infty} \frac{1}{K_n^A} [\alpha_n^A I_{ni}^e(y) + \alpha_n^A I_{ni}^h(y)] \cdot \sin \alpha_n^A(x + A) e^{-j\beta z} \tag{1d}$$

$$E_{zi}(x, y, z) = \sum_{n=1}^{\infty} \frac{1}{K_n^A} [j\beta V_{ni}^e(y) + \alpha_n^A V_{ni}^h(y)] \cdot \sin \alpha_n^A(x + A) e^{-j\beta z} \tag{1e}$$

$$H_{zi}(x, y, z) = \sum_{n=1}^{\infty} \frac{1}{K_n^A} [j\beta I_{ni}^e(y) + j\beta I_{ni}^h(y)] \cdot \cos \alpha_n^A(x + A) e^{-j\beta z} \tag{1f}$$

$$K_n^A = \sqrt{\alpha_n^{A^2} + \beta^2}, \quad \alpha_n^A = \frac{(n - 1/2)\pi}{A}, \quad i = 1, 3, 4 \tag{1g}$$

and

$$E_{y2}(x, y, z) = \frac{1}{j\omega\epsilon_2} \sum_{n=1}^{\infty} K_n^w I_{ni}^e(y) \sin \alpha_n^w(x + s) e^{-j\beta z} \tag{2a}$$

$$H_{y2}(x, y, z) = \frac{1}{j\omega\mu_2} \sum_{n=1}^{\infty} K_n^w V_{ni}^h(y) \cos \alpha_n^w(x + s) e^{-j\beta z} \tag{2b}$$

$$E_{x2}(x, y, z) = \sum_{n=1}^{\infty} \frac{-1}{K_n^w} [\alpha_n^w V_{ni}^e(y) + j\beta V_{ni}^h(y)] \cdot \cos \alpha_n^w(x + s) e^{-j\beta z} \tag{2c}$$

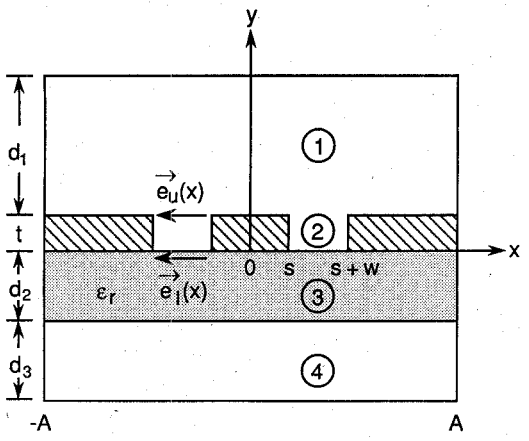

Fig. 2. Transverse cross section of a CPW with thick metallization. Eigenmodes of this CPW structure are derived as an example.

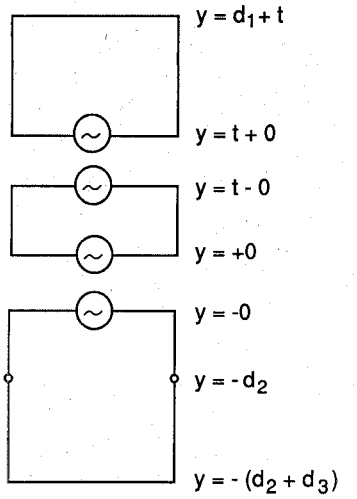

Fig. 3. Equivalent circuit of the structure of Fig. 2 in the y-direction. The mode voltages and currents are derived in terms of the aperture electric fields $\vec{e}_u(x)$ and $\vec{e}_l(x)$ by applying the circuit theory to this equivalent circuit.

$$H_{x2}(x, y, z) = \sum_{n=1}^{\infty} \frac{1}{K_n^w} [j\beta V_{ni}^e(y) + \alpha_n^w V_{ni}^h(y)] \cdot \sin \alpha_n^w(x + s) e^{-j\beta z} \quad (2d)$$

$$E_{z2}(x, y, z) = \sum_{n=1}^{\infty} \frac{1}{K_n^w} [j\beta V_{ni}^e(y) + \alpha_n^w V_{ni}^h(y)] \cdot \sin \alpha_n^w(x + s) e^{-j\beta z} \quad (2e)$$

$$H_{z2}(x, y, z) = \sum_{n=1}^{\infty} \frac{1}{K_n^w} [\alpha_n^w I_{ni}^e(y) + j\beta I_{ni}^h(y)] \cdot \cos \alpha_n^w(x + s) e^{-j\beta z} \quad (2f)$$

$$K_n^w = \sqrt{\alpha_n^{w2} + \beta^2}, \quad \alpha_n^w = \frac{n\pi}{w} \quad (2g)$$

where β is the propagation constant which is real for propagating modes and imaginary for evanescent modes. The mode voltages $V_{ni}^r(y)$ and currents $I_{ni}^r(y)$, $r = e, h$, are derived by applying conventional circuit theory to the equivalent circuit in the y direction (Fig. 3) [28].

The mode voltages and currents can be expressed in terms of the Fourier transforms of the unknown aperture electric fields, $\tilde{e}_{ux}$, $\tilde{e}_{uz}$, $\tilde{e}_{lx}$ and $\tilde{e}_{lz}$, after some mathematical manipulations. Finally, the condition that magnetic fields need to be continuous across the boundaries $y = t$ and $y = 0$ is imposed. A system of equations relating the Fourier transforms of unknown aperture electric fields and surface current distribution $\tilde{J}_{ux}$, $\tilde{J}_{uz}$, $\tilde{J}_{lx}$ and $\tilde{J}_{lz}$ on the top and bottom surfaces of the metallization can be written as

$$\begin{bmatrix} G_{11} & G_{12} & G_{13} & G_{14} \\ G_{21} & G_{22} & G_{23} & G_{24} \\ G_{31} & G_{32} & G_{33} & G_{34} \\ G_{41} & G_{42} & G_{43} & G_{44} \end{bmatrix} \begin{bmatrix} \tilde{e}_{ux} \\ \tilde{e}_{ux} \\ \tilde{e}_{lx} \\ \tilde{e}_{lz} \end{bmatrix} = \begin{bmatrix} \tilde{J}_{ux} \\ \tilde{J}_{uz} \\ \tilde{J}_{lx} \\ \tilde{J}_{lz} \end{bmatrix} \quad (3)$$

where G_{ij}'s $(i, j = 1, 2, 3, 4)$ are the Green's functions. In the numerical calculation, the unknown aperture electric fields $\vec{e}_u(x)$ and $\vec{e}_l(x)$ are expanded in terms of appropriate basis functions which incorporate the edge condition. The following basis functions are chosen:

$$\frac{T_{k-1}\left(\dfrac{x - s - w/2}{w/2}\right)}{\sqrt{1 - \left(\dfrac{x - s - w/2}{w/2}\right)}}, \quad k = 1, 2, \cdots, P \quad (4)$$

for the x component and

$$U_{k-1}\left(\frac{x - s - w/2}{w/2}\right), \quad k = 1, 2, \cdots, Q \quad (5)$$

for the z component of the aperture electric fields. $T_k(x)$ and $U_k(x)$ are the Chebyshev polynomials of the first and second kinds, respectively. The final determinant equation for the unknown propagation constant is obtained by applying the Galerkin's procedure to (3) to lead to a set of $P + Q$ linear homogeneous equations. Nontrivial solutions of this set of equations decide the propagation constant β and the modal field distributions associated with β.

III. Mode-Matching Technique

The mode-matching procedure is briefly described in this section. Electromagnetic fields to both sides of the discontinuity are expanded by using the eigenmodes of the individual transmission lines. Assuming the incident waves comes from the left side of the discontinuity, $z = -\infty$, toward the junction discontinuity located at $z = 0$, (see Fig. 1), the transverse electric and magnetic fields inside the left waveguide a can be expressed as the superposition of the incident and all the reflected waves:

$$\vec{E}_{at}(x, y, z) = \vec{e}_{a1}(x, y) e^{-j\beta_{a1} z} + \sum_{n=1}^{\infty} a_n \vec{e}_{an}(x, y) e^{+j\beta_{an} z}, \quad z < 0 \quad (6a)$$

$$\vec{H}_{at}(x, y, z) = \vec{h}_{a1}(x, y)\, e^{-j\beta_{a1} z} - \sum_{n=1}^{\infty} a_n \vec{h}_{an}(x, y)\, e^{+j\beta_{an} z} \tag{6b}$$

where $\vec{e}_{an}(x, y)$ and $\vec{h}_{an}(x, y)$ are the eigenmodes of the left waveguide a and a_n's are the unknown expansion coefficients. β_{a1} is the propagation constant of the incident wave. The corresponding transverse electromagnetic fields in the right waveguide are written as

$$\vec{E}_{bt}(x, y, z) = \sum_{m=1}^{\infty} b_m \vec{e}_{bm}(x, y)\, e^{-j\beta_{bm} z} \tag{7a}$$

$$z > 0$$

$$\vec{H}_{bt}(x, y, z) = \sum_{m=1}^{\infty} b_m \vec{h}_{bm}(x, y)\, e^{-j\beta_{bm} z} \tag{7b}$$

where $\vec{e}_{bm}(x, y)$ and $\vec{h}_{bm}(x, y)$ are the eigenmodes of the left waveguide b and b_m's are the unknown expansion coefficients. The tangential electromagnetic fields need to be continuous across the $z = 0$ plane where the junction discontinuity is located at, therefore,

$$\vec{e}_{a1}(x, y) + \sum_{n=1}^{\infty} a_n \vec{e}_{an}(x, y) = \sum_{m=1}^{\infty} b_m \vec{e}_{bm}(x, y) \tag{8a}$$

$$\vec{h}_{a1}(x, y) - \sum_{n=1}^{\infty} a_n \vec{h}_{an}(x, y) = \sum_{m=1}^{\infty} b_m \vec{h}_{bm}(x, y). \tag{8b}$$

In order to determine the unknown coefficients a_n and b_m, an inner product needs to be defined to eliminate the x, y dependence in (8) and lead to a system of linear equations. An inner product defined as

$$I_{nm}^{ab} = \langle \vec{e}_{an}(x, y), \vec{h}_{bm}(x, y) \rangle = \int_S \vec{e}_{an}(x, y) \times \vec{h}_{bm}(x, y) \cdot d\vec{s} \tag{9}$$

is introduced, where S is the cross section of the rectangular waveguide shield. The inner product is defined according to the boundary enlargement type waveguide discontinuity [30]. For this type of discontinuity problem, the electric field for the inner product is taken from the waveguide which has smaller aperture while the magnetic field is taken from the waveguide which has larger aperture. For the structures shown in Fig. 1(a)–(c), the electric field from the left waveguide a and magnetic field from the right waveguide b are used in (9) for the inner product calculation. Inner product defined in this manner obtains convergent solutions with minimum number of modes [17] compared to inner product defined otherwise. The inner product defined by (9) for the mode-matching procedure also represents the concept of interaction between different modes either from the same waveguide or different waveguides. Performing the inner products on (8) results in a system of equations as

$$\sum_{n=1}^{N_a} a_n I_{ni}^{ab} - \sum_{m=1}^{N_b} b_m I_{mi}^{bb} = -I_{1i}^{ab}, \qquad i = 1, 2, \cdots, N_b \tag{10a}$$

$$\sum_{n=1}^{N_a} a_n I_{jn}^{aa} + \sum_{m=1}^{N_b} b_m I_{jm}^{ab} = I_{j1}^{aa}, \qquad j = 1, 2, \cdots, N_a \tag{10b}$$

Theoretically, an infinite number of modes need to be used on both sides of the junction to account for the discontinuity. However, in actual numerical computation, only a finite number of modes, N_a and N_b, are used for each waveguide. Since the conducting walls of the outside rectangular waveguide shield are perfect conductors, the eigenmodes of each shielded transmission line should satisfy the mode orthogonality relation:

$$I_{jn}^{aa} = \int_S \vec{e}_{aj}(x, y) \times \vec{h}_{an}(x, y) \cdot d\vec{s} = \delta_{jn} \tag{11a}$$

$$I_{mi}^{bb} = \int_S \vec{e}_{bm}(x, y) \times \vec{h}_{bi}(x, y) \cdot d\vec{s} = \delta_{mi} \tag{11b}$$

where δ_{jm} and δ_{mi} are the Kronecker delta functions. As a result of (11), the computation work of (10) is greatly reduced if the eigenmodes of each transmission line are normalized first. The system of equations (10) is then solved for the unknown expansion coefficients which for the dominant incident wave the reflection coefficient $S_{11} = a_1$ and transmission coefficient $S_{21} = b_1$.

IV. Numerical Results

A computer program based on the mode-matching procedure described above was developed. The program analyzes the junction discontinuities of CPW as well as finline. This is achieved by simply changing the basis functions for the aperture electric fields and the structural symmetry of a magnetic wall at $x = 0$ for CPW to a electric wall for finline. Extensive convergence tests were performed to study the convergence behavior of the numerical results. The outside shielding used for all the numerical calculations is the WR-28 rectangular waveguide, i.e., $2A = 3.556$ mm and $d_1 + t + d_2 + d_3 = 7.118$ mm. The data presented in this paper were all calculated with 6 eigenmodes, i.e., $N_a = N_b = 6$. The relative error between the cases when 6 and 7 eigenmodes are used is only 0.5% within the freqency range of interest. Since the transmission lines on both sides of the junction discontinuity are inside the same rectangular waveguide shield, the cross sections of each guide are the same. Therefore, the "relative convergence" [15], [31] problem is not a factor in the numerical computation of the structure studied here and equal number of modes are used in both sides of the discontinuity. Other requirements were also checked to validate the numerical results. Power conservation ($|S_{11}|^2 + |S_{21}|^2 = 1$) and reciprocity ($S_{21} = S_{12}$) conditions are both satisfied to within 0.01% of error, although they are only the necessary conditions but not the sufficient conditions for the results to be correct.

The reflection and transmission coefficients of a unilateral finline step discontinuity without metallization thick-

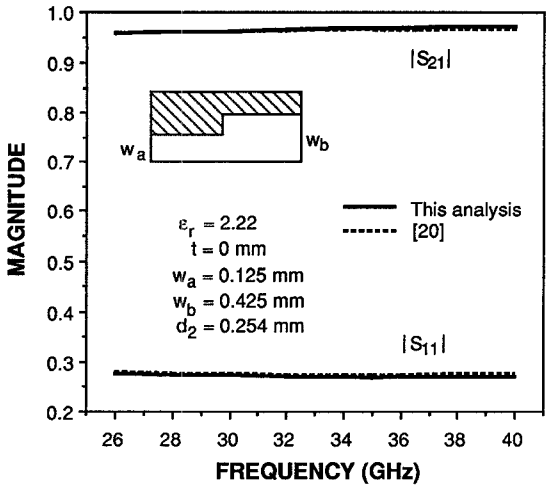

Fig. 4. Comparison of numerical results obtained in this paper with existing data for a finline step discontinuity without metallization thickness.

ness are first calculated and compared with existing data to confirm the accuracy of the numerical results. The results are plotted in Fig. 4. Agreement between our data and those in [20] is very good. Magnitude of scattering parameters of the same finline step discontinuity with different metallization thickness are demonstrated in Fig. 5(a). It is interesting to note that the reflection coefficient decreases as the metallization thickness t increases. A possible explanation of this phenomenon is that the region between the top and bottom surface of the metallization actually behaves like a parallel-plate waveguide. When the metallization thickness increases, there is more energy being transmitted along this parallel-plate waveguide region and the transmission coefficient increases accordingly. Therefore, the reflection coefficient $|S_{11}|$ will decrease as the metallization thickness t increases. Phase of the scattering parametrs of this finline step discontinuity is shown in Fig. 5(b).

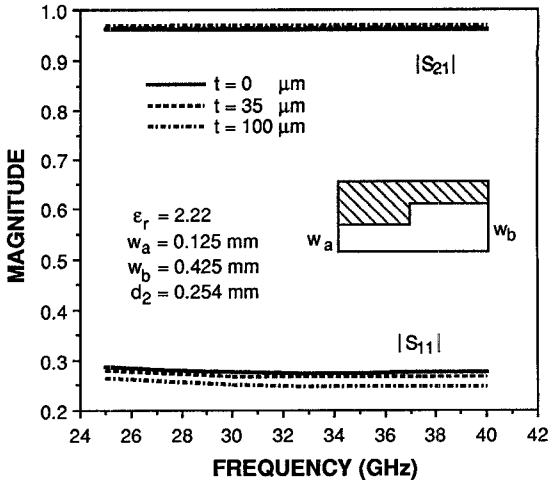

(a)

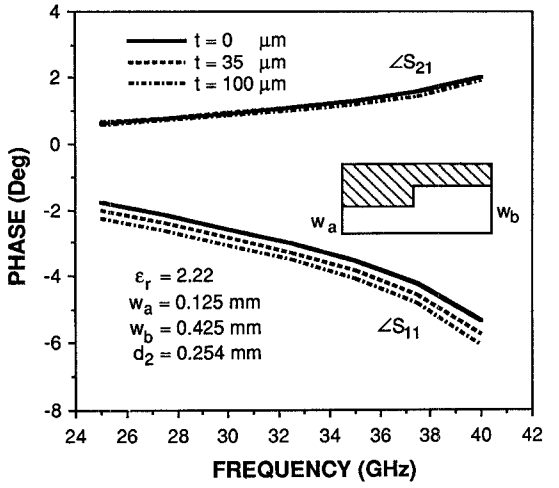

(b)

Fig. 5. Scattering parameters of the same finline step discontinuity as in Fig. 4 with different metallization thickness. (a) Magnitude. (b) Phase.

Fig. 6(a) shows the magnitude of scattering parameters of the shielded CPW step discontinuity. While the effect of finite metallization thickness on the finline step discontinuity is obvious throughout the frequency range of interest, finite metallization thickness affects the reflection coefficient of CPW step discontinuity significantly only at high frequency range. Magnitude of the reflection coefficient is also inversely proportional to the metallization thickness, as in the case of a finline step discontinuity. Phases of the reflection and transmission coefficients of the CPW step discontinuity are plotted in Fig. 6(b).

The CPW-finline transition structure in Fig. 1(c) can be excited in two different modes. The odd-mode excitation is obtained by placing a magnetic wall at $x = 0$ and excites the CPW modes for the transmission line on the left side of the transition and odd modes for the other line. Even-mode excitation is obtained by replacing the magnetic wall at $x = 0$ with an electric wall. Coupled-slot modes and the normal finline modes are excited for the transmission lines on left and right sides, respectively, of the transition. Fig. 7(a) shows the magnitudes of scattering parameters with the CPW mode excitation for the transition structure. CPW modes and the odd finline modes are virtually uncoupled, $|S_{21}| \sim 0.003$, when the metallization thickness is zero. Phase (Fig. 7(b)) for the reflection coefficient is always 180° and phase for the transmission coefficient is always 0°. The data indicate that the transition is actually an open circuit, which is predictable. However, in real situation when the metallization thickness is not zero, some amount of power is coupled from the CPW side to the finline side, as is depicted in Fig. 7(a). Numerical results for the coupled-slot mode excitation are plotted in Fig. 8. Unlike the CPW mode excitation, there is always certain amount of power coupled from the coupled slotline to the finline. This result is also predictable by comparing the aperture field configurations of the individual coupled-slot line and finline.

Figs. 9 and 10 show the numerical results of a different transition structure. The gaps between the ground plane and the center strip are narrower and the center strip is wider in this case and the dielectric constant is also different. The transition structure under the CPW mode ex-

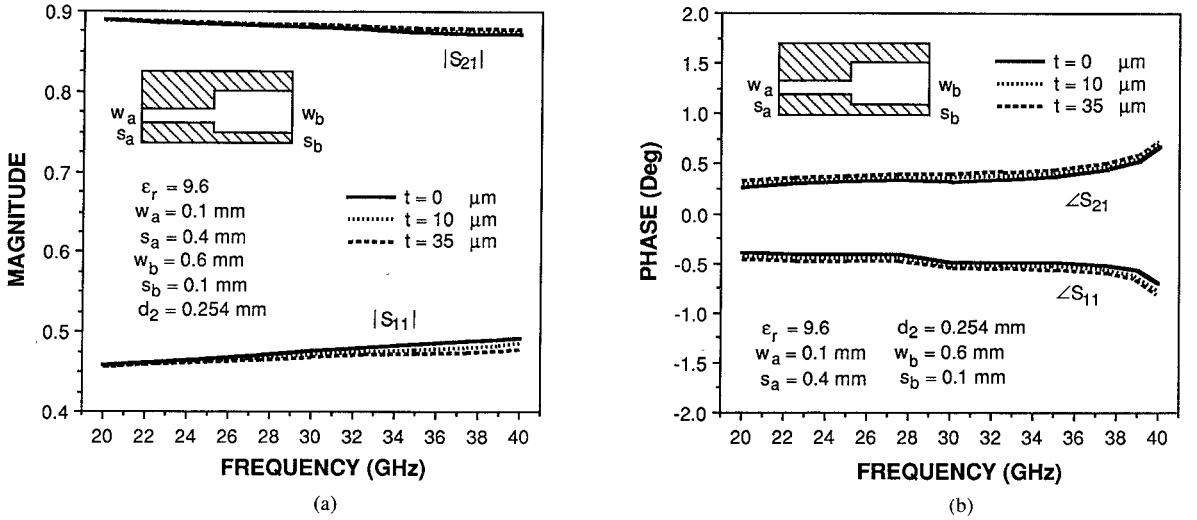

(a) (b)

Fig. 6. Scattering parameters of the CPW step discontinuity with different metallization thickness. (a) Magnitude. (b) Phase.

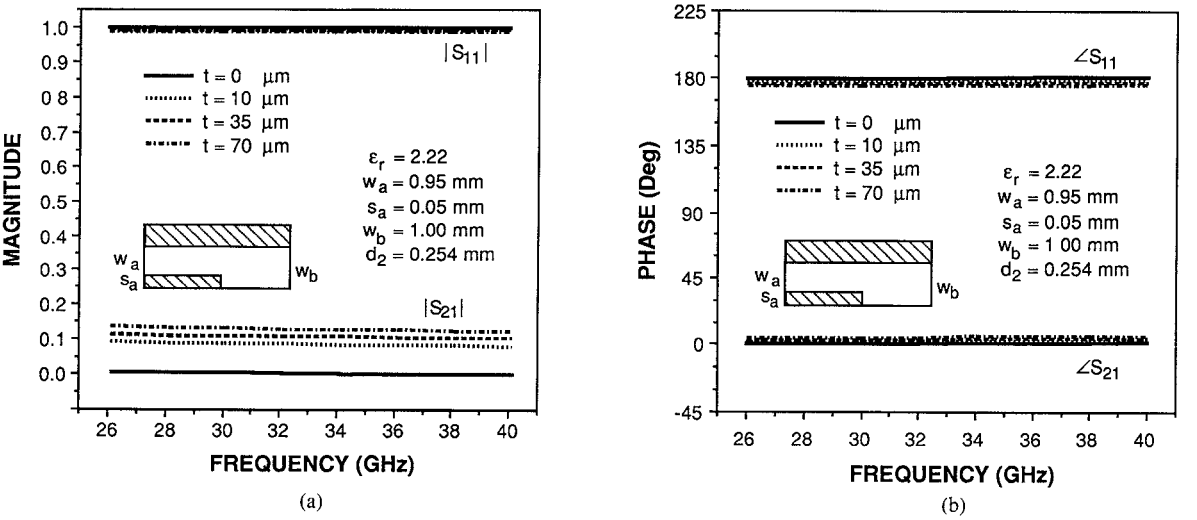

(a) (b)

Fig. 7. Scattering parameters of the CPW-finline transition for odd-mode excitation with different metallization thickness. (a) Magnitude. (b) Phase.

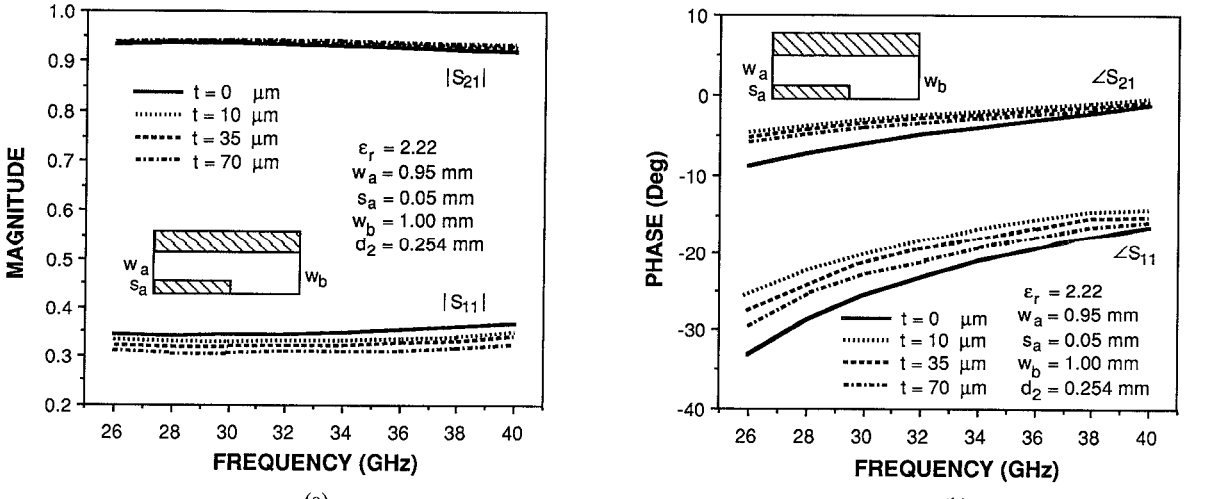

(a) (b)

Fig. 8. Scattering parameters of the same CPW-finline transition as in Fig. 7 for even-mode excitation with different metallization thickness. (a) Magnitude. (b) Phase.

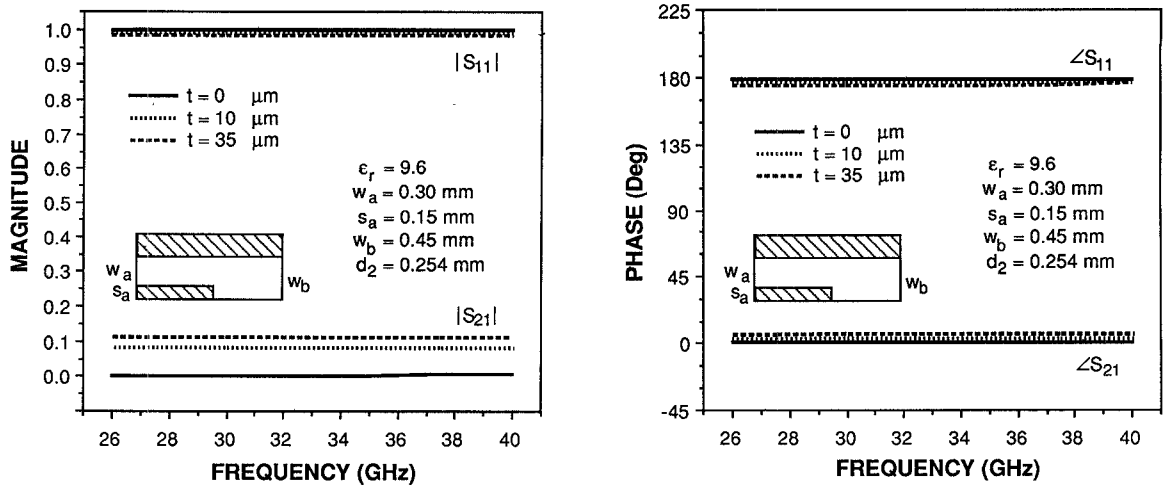

Fig. 9. Numerical results for a CPW-finline transition with odd-mode excitation. (a) Magnitude. (b) Phase. The center strip of the CPW is wider in this case.

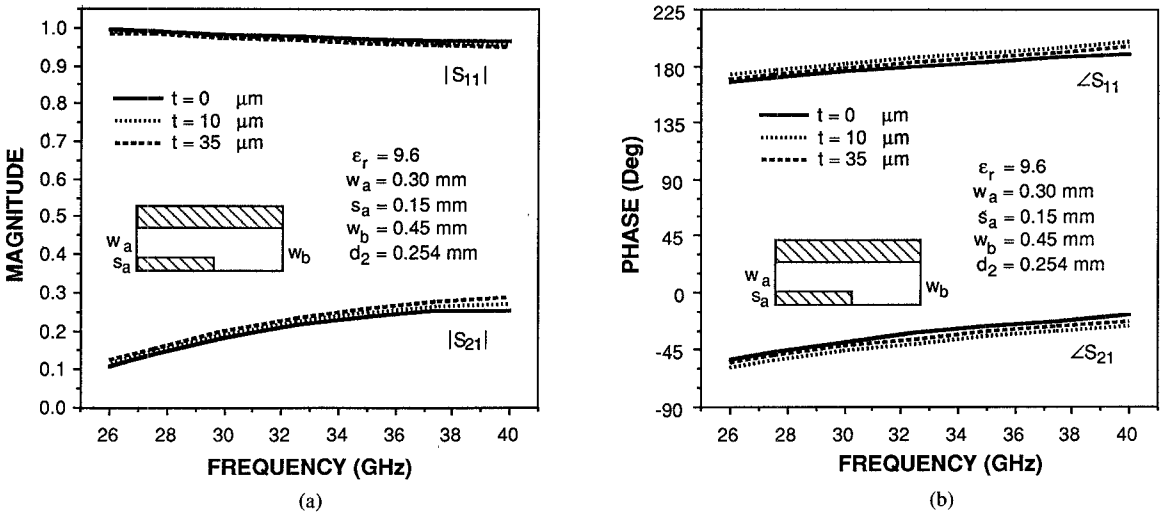

Fig. 10. Scattering parameters of the same CPW-finline transition as in Fig. 9 with even-mode excitation. (a) Magnitude. (b) Phase.

citation always demonstrates the characteristics of an open circuit no matter how large the discontinuity is in terms of size, as is shown in Fig. 9. When there is actually coupling between the two transmission lines as in the coupled-slot mode excitation, the discontinuity affects the reflection and transmission coefficients. Since the structural discontinuity in Fig. 10 is larger than that in Fig. 8, it is expected that the transmission coefficient should be smaller in this case. Comparison of Fig. 10(a) with Fig. 8(a) confirms this assumption.

V. Conclusion

Shielded coplanar type transmission line junction discontinuities including the finite metallization thickness effect were studied by using the mode-matching technique. Numerical results for several discontinuity structures, specifically, finline step discontinuity, CPW step discontinuity and CPW-finline transition with odd- and even-mode excitations, were presented for the first time with the finite metallization thickness being considered. Comparison with previously published data and convergence tests were performed to confirm the accuracy of the numerical results. The method is versatile and in principle can also handle the microstrip line junction discontinuities. An extension of the present work will involve the characterization of more complicated junction discontinuities between coplanar type transmission lines.

Acknowledgment

The authors would like to thank Dr. T. Kitazawa of Kitami Institute of Technology, Japan, for helpful suggestions and discussions.

References

[1] T. Itoh and R. Mittra, "Spectral-domain approach for calculating the dispersion characteristics of microstrip lines," *IEEE Trans. Microwave Theory Tech.*, vol. MTT-21, pp. 496–499, July 1973.

[2] R. H. Jansen, "Hybrid mode analysis of end effects of planar microwave and millimeter wave transmission line," *Proc. Inst. Elec. Eng.*, pt. H, vol. 128, pp. 77–86, 1981.
[3] R. H. Jansen and N. H. L. Koster, "Some new results on the equivalent circuit parameters of the inductive strip discontinuity in unilateral finlines," *Arch. Elek. Übertragung.*, pp. 497–499, 1981.
[4] J. B. Knorr, "Equivalent reactance of a shorting septum in a finline: Theory and experiment," *IEEE Trans. Microwave Theory Tech.*, vol. MTT-29, pp. 1196–1202, Nov. 1981.
[5] J. B. Knorr and J. C. Deal, "Scattering coefficients of an inductive strip in a finline: Theory and experiment," *IEEE Trans. Microwave Theory Tech.*, vol. MTT-33, pp. 1011–1017, Oct. 1985.
[6] R. H. Jansen and N. H. L. Koster, "A unified CAD basis for the frequency dependent characterization of strip, slot and coplanar MIC components," in *Proc. 11th European Microwave Conf.*, 1981, pp. 682–687.
[7] N. H. L. Koster and R. H. Jansen, "The equivalent circuit of the asymmetrical series gap in microstrip and suspended-substrate line," *IEEE Trans. Microwave Theory Tech.*, vol. MTT-30, pp. 1273–1279, Aug. 1982.
[8] ——, "The microstrip step discontinuity: A revised description," *IEEE Trans. Microwave Theory Tech.*, vol. MTT-34, pp. 213–223, Feb. 1986.
[9] R. E. Collin, *Field Theory of Guided Waves*. New York: McGraw-Hill, 1960.
[10] R. Sorrentino and T. Itoh, "Transverse resonance analysis of finline discontinuities," *IEEE Trans. Microwave Theory Tech.*, vol. MTT-32, pp. 1632–1638, Dec. 1984.
[11] H. Y. Yang and N. G. Alexopoulos, "Characterization of the finline step discontinuity on anisotropic substrates," *IEEE Trans. Microwave Theory Tech.*, vol. MTT-35, pp. 956–963, Nov. 1967.
[12] A. Biswas and B. Bhat, "Accurate characterization of an inductive strip in finline," *IEEE Trans. Microwave Theory Tech.*, vol. 36, pp. 1233–1238, Aug. 1988.
[13] R. F. Harrington, *Time-Harmonic Electromagnetic Fields*. New York: McGraw-Hill, 1961.
[14] T. S. Chu and T. Itoh, "Generalized scattering matrix method for analysis of cascaded and offset microstrip step discontinuities," *IEEE Trans. Microwave Theory Tech.*, vol. MTT-34, pp. 280–284, Feb. 1984.
[15] T. S. Chu, T. Itoh, and Y. C. Shih, "Comparative study of mode matching formulations for microstrip discontinuity problems," *IEEE Trans. Microwave Theory Tech.*, vol. MTT-33, pp. 1018–1023, Oct. 1985.
[16] N. K. Uzunoglu, C. N. Capsalis, and C. P. Chronopoulos, "Frequency-dependent analysis of a shielded microstrip step discontinuity using an efficient mode-matching technique," *IEEE Trans. Microwave Theory Tech.*, vol. MTT-36, pp. 976–984, June 1988.
[17] Q. Zu, K. J. Webb, and R. Mittra, "Study of modal solution procedures for microstrip step discontinuities," *IEEE Trans. Microwave Theory Tech.*, vol. MTT-37, pp. 381–387, Feb. 1989.
[18] H. El Hennawy and K. Schünemann, "Analysis of finline discontinuities," in *Proc. 9th European Microwave Conf.* Brighton, England, 1979, pp. 448–452.
[19] K. Uhde, "Discontinuities in finlines on semiconductor substrate," *IEEE Trans. Microwave Theory Tech.*, vol. MTT-34, pp. 1499–1507, Dec. 1984.
[20] M. Helard, J. Citerne, O. Picon, and V. F. Hanna, "Theoretical and experimental investigation of finline discontinuities," *IEEE Trans. Microwave Theory Tech.*, vol. MTT-33, pp. 994–1003, Oct. 1985.
[21] K. J. Webb and R. Mittra, "Solution of the finline step-discontinuity problem using the generalized variational technique," *IEEE Trans. Microwave Theory Tech.*, vol. MTT-33, pp. 1004–1010, Oct. 1985.
[22] O. Picon, V. F. Hanna, J. Citerne and J.-P. Lefevre, "Exact calculation of scattering parameters of the coplanar-slot transition in unilateral finline technology," *IEEE Trans. Microwave Theory Tech.*, vol. MTT-35, pp. 1408–1413, Dec. 1987.
[23] M. Naghed and I. Wolff, "Equivalent capacitance of coplanar waveguide discontinuities and interdigitated capacitors using a three-dimensional finite difference method," *IEEE Trans. Microwave Theory Tech.*, vol. 38, pp. 1808–1815, Dec. 1990.
[24] R. A. Pucel, "Design considerations for monolithic microwave circuits," *IEEE Trans. Microwave Theory Tech.*, vol. MTT-29, pp. 513–534, Apr. 1981.
[25] T. Hirota, T. Tarusawa and H. Ogawa, "Uniplanar MMIC hybrids: A proposed new MMIC structure," *IEEE Trans. Microwave Theory Tech.*, vol. MTT-35, pp. 576–581, June 1987.
[26] L. W. Dikens, and D. W. Maki, "An integrated-circuit balanced mixer, image and sum enhanced," *IEEE Trans. Microwave Theory Tech.*, vol. MTT-23, pp. 276–281, Mar. 1975.
[27] U. H. Gysel, "A 26.5-to-40-GHz planar balance mixer," in *Proc. 5th European Microwave Conf.*, Hamburg, 1975, pp. 491–495.
[28] T. Kitazawa and Y. Hayashi, "Quasistatic and hybrid-mode analysis of shielded coplanar waveguide with thick metal coating," *Proc. Inst. Elec. Eng.*, vol. 134, pt. H, no. 3, June 1987.
[29] T. Kitazawa and R. Mittra, "Analysis of finline with finite metallization thickness," *IEEE Trans. Microwave Theory Tech.*, vol. MTT-32, pp. 1484–1487, Nov. 1984.
[30] A. Wexler, "Solution of waveguide discontinuities by modal analysis," *IEEE Trans. Microwave Theory Tech.*, vol. MTT-15, pp. 508–517, Sept. 1967.
[31] R. Mittra and S. W. Lee, *Analytical Techniques in the Theory of Guided Waves*. New York: Macmillan, 1971.

Chih-Wen Kuo was born in Kaohsiung, Taiwan, R.O.C., on June 11, 1964. He received the B.Sc. degree in electrical engineering from National Taiwan University in 1986.

From 1986 to 1987, he was employed as a Research Assistant in the Institute of Information Science, Academia Sinica, Taiwan, R.O.C. In September of 1987, he joined the graduate school of the University of Texas at Austin and obtained the M.Sc. and Ph.D. degrees in Electrical Engineering in 1989 and 1991, respectively. His research interests involve the loss calculations of planar transmission line structures and the characterization of discontinuities between planar transmission lines.

Tatsuo Itoh (S'69–M'69–SM'74–F'82) received the Ph.D. degree in Electrical Engineering from the University of Illinois, Urbana in 1969.

From September 1966 to April 1976, he was with the Electrical Engineering Department, University of Illinois. From April 1976 to August 1977, he was a Senior Research Engineer in the Radio Physics Laboratory, SRI International, Menlo Park, CA. From August 1977 to June 1978, he was an Associate Professor at the University of Kentucky, Lexington. In July 1978, he joined the faculty at the University of Texas at Austin, where he became a Professor of Electrical Engineering in 1981 and Director of the Electrical Engineering Research Laboratory in 1984. During the summer of 1979, he was a Guest Researcher at AEG-Telefunken, Ulm, West Germany. In September 1983, he was selected to hold the Hayden Head Centennial Professorship of Engineering at The University of Texas. In September 1984, he was appointed Associate Chairman for Research and Planning of the Electrical and Computer Engineering Department at The University of Texas. In January 1991, he joined the University of California, Los Angeles as Professor of Electrical Engineering and holder of the TRW Endowed Chair in Microwave and Millimeter Wave Electronics.

Dr. Itoh is a member of the Institute of Electronics and Communication Engineers of Japan, Sigma Xi, and Commissions B and D of USNC/URSI. He served as Editor of IEEE TRANSACTIONS ON MICROWAVE THEORY AND TECHNIQUES for 1983–1985 and currently serves on the Administrative Committee of IEEE Microwave Theory and Techniques Society. He was Vice President of the Microwave Theory and Techniques Society in 1989 and President in 1990. He is the Editor-in-Chief of IEEE MICROWAVE AND GUIDED WAVE LETTERS. He was the Chairman of USNC/URSI Commission D from 1988 to 1990 and is the Vice-Chairman of Commission D of the International URSI.